Acta Agrophysica, 2002, 80, 181-193

APPLICATION OF LIF TECHNIQUE FOR THE SPACE- AND TIME-RESOLVED MONITORING OF POLLUTANT GAS DECOMPOSITION IN NON-THERMAL PLASMA REACTORS

J. Mizeraczyk, T. Ohkubo, S. Kanazawa*, M. Kocik*

Centre of Plasma and Laser Engineering, Institute of Fluid Flow Machinery, Polish Academy of Sciences, 80-231 Gdańsk, Fiszera 14, Poland, jmiz@imp.gda.pl

*Department of Electrical and Electronic Engineering, Oita University, 700 Dannoharu, Oita, Japan 870-1192, tohkubo@cc.oita-u.ac.jp

A b s t r a c t. Laser-induced fluorescence (LIF) technique aided by intensified CCD light signal detection and fast digital image processing is demonstrated to be a useful diagnostic method for *in-situ* observation of the discharge-induced plasma-chemistry processes responsible for NO_x ($NO + NO_2$) decomposition occurring in non-thermal plasma reactors. In this paper a method and results of the LIF measurement of two-dimensional distribution of the ground-state NO molecule density inside a DC positive streamer corona reactor during NO removal from a flue gas simulator [air/NO(up to 300 ppm)] are presented. The obtained results showed that the corona discharge-induced removal of NO molecules occurred not only in the vicinity of the plasma region formed by the corona streamers and in the downstream region of the reactor but also in the upstream region of the reactor, i.e. before the flue gas simulator has entered the plasma region. This information, obtained owing to the LIF technique, is important for the understanding of the plasma-chemistry processes responsible for NO_x decomposition in non-thermal plasma reactors and for optimising their performance.

K e y w o r d s: LIF diagnostics, corona discharge, NO_x, NO_x abatement, non-thermal plasma reactor.

INTRODUCTION

The space- and time-resolved pictures of gas-dynamic processes have become crucial for the detailed understanding of the pulsed or transient electrical discharge and plasma processes. An example is the DC and pulsed corona discharges which nowadays have recovered interest because of their potential for the decomposition of gaseous pollutants in the exhaust gases. Although both corona discharges have been studied for dozens of years, they are still not fully understood because of their complex nature involving transient plasma and gas-dynamic processes together with complicated chemistry. Full understanding of the processes occurring in the corona discharges is indispensable for improving its performance in order to increase the efficiency of the gaseous pollutant processing in the exhaust gases.

Up to now several modern computer codes have been created for modelling the plasma, gas-dynamic and chemical processes in the corona discharges [1-7]. However, they are reliable only to some extend because of the complexity of phenomena involved and lack of experimental data which could support and verify the codes.

Recent technological progress in the developments of tunable excimer lasers (TEL), intensified CCD (ICCD) cameras, imaging spectrographs and fast digital image processing has made laser diagnostics of complex gaseous media possible with higher sensitivity and space and time resolution than ever. An advantage of TELs is that they can be employed in almost every laser-based diagnostic method including the diagnostics based on Mie, Rayleigh and Raman scattering, laser induced fluorescence (LIF) and particle image velocimetry. A comprehensive review of the state of the art of the application of the TELs to diagnostics of the gas-dynamic processes in combustion was given by Rothe and Andresen [8]. The review demonstrated that nowadays the TEL diagnostics are being used as a high sensitive technique to produce species-, space-, and time-resolved images of complex turbulent flows in many combustion devices, including the complex gas dynamics in an internal combustion engine. Rothe and Andresen suggested that the TEL diagnostics is suitable and convenient for basic and applied studies of many other transient or turbulent media, including those in electrical discharge and plasma devices. In particular, it concerns the LIF method which is a very efficient technique for measuring concentrations of species in dynamic and transient conditions occurring in the corona discharges.

The corona discharge plasma processing used for NO_x ($NO + NO_2$) removal from the flue gases has been studied either numerically using plasma-chemistry models [1-7] or experimentally (e.g. [9, 10]). However, there is still a lack of fundamental data to develop a comprehensive model of the plasma-chemistry processes, which would satisfactory describe NO_x removal from the flue gases. This makes the understanding of the corona discharge-induced chemical reactions responsible for NO_x removal difficult and hinders improving the efficiency of NO_x removal. The spatial and time distribution of NO molecule density in the reactor is crucial for understanding the NO_x removal. However, in the most experimental investigations on NO_x removal by the corona discharge plasmas, NO density was measured using conventional NO monitors based on chemi-luminescence, infrared absorption, or potentiostatic electrolysis, placed at the outlet of the reactor. Such measurements did not provide information on the spatial and time distribution of NO molecule density in the reactor and, in particular, in the discharge region. Therefore, they are not much informative when the kinetics of the plasma-chemistry processes in the corona discharge and reactor is considered.

In this paper, results of the LIF measurement of two-dimensional distribution of the ground-state NO molecule density in a steady-state high-repetition DC corona discharge between a 3-cm gap electrode arrangement (needle-to-plate or nozzle-to-plate) in NO/air mixture are presented.

EXPERIMENTAL METHOD AND APPARATUS

Our investigation was aimed at measuring NO density distribution in a non-thermal plasma reactor in which the high-repetition rate (about 5 kHz) DC corona discharge in a 3-5 cm gap between either the needle-to-plane or nozzle-to-plate electrode arrangement was used for NO removal from a flue gas simulator [NO (up to 300 ppm)/air]. The LIF technique was employed for monitoring NO molecules under the steady-state DC corona discharge condition. This was an essential difference to the previous investigations [11-19] in which the LIF monitoring of NO molecules (or OH radicals) was carried out either after the single transient discharge or between two discharge pulses with a relatively long interval between them (low-repetition pulsed discharges, e.g. 10 Hz).

The laser induced fluorescence on the NO ($X^2\Pi(v''=0) \leftarrow A^2\Sigma^+ (v'=0)$) transition was chosen for the monitoring of the ground-state NO molecules, which prevail among the NO molecules in the corona discharge. This transition was induced by the irradiation of NO molecules with UV laser pulses of a wavelength of 226 nm generated by a LIF system consisted of a XeF excimer laser, dye laser and BBO crystal (Fig. 1). The laser pulses from the XeF excimer laser (Lambda Physik, Compex 150, tuned at 351 nm) pumped a dye laser (Lambda Physik, Scanmate) with Coumarin 47 as a dye, which generated the laser beam of a wavelength tunable around 450 nm. Then, the dye laser beam pumped a BBO crystal in which the second harmonic radiation of a wavelength correspondingly tunable around 226 nm was generated. The 226-nm UV laser beam pulses of energy of 0.8-2 mJ and duration of about 20 ns were transformed with a cylindrical lens-spherical lens system into the form of the so-called laser sheet (width of 1 mm, height of about 30 mm), which passed between the electrodes in the reactor. Thus, the energy density of the laser sheet pulses could reach 6.7 mJ/cm^2.

The reactor was an acrylic box (100mm x 125mm x 700mm) in which quartz windows were mounted for transmission of the laser pulses and the LIF signal detection. To minimize the scattered light, the laser pulses were absorbed in a beam dumper placed at rear of the reactor (Fig. 1). Either the conventional needle-to-plane or the nozzle-to-plate electrode arrangement was used (Fig. 2.). The needle electrode was made of a brass rod (6 mm in diameter), the end of which had a tapered profile with the tip of a radius of curvature of 0.5 mm. The nozzle electrode was made of a stainless-steal pipe of an inner and outer diameter of 1.0 mm and 1.5

mm, respectively. The grounded electrode was a stainless-steel plate. The distance between the stressed and grounded electrode was equal to 30 mm. DC high voltage with positive polarity was applied through a 10-MΩ resistor to the stressed electrode. Two corona discharge modes, either glow corona or streamer corona could be generated in the gap, depending on applied voltage.

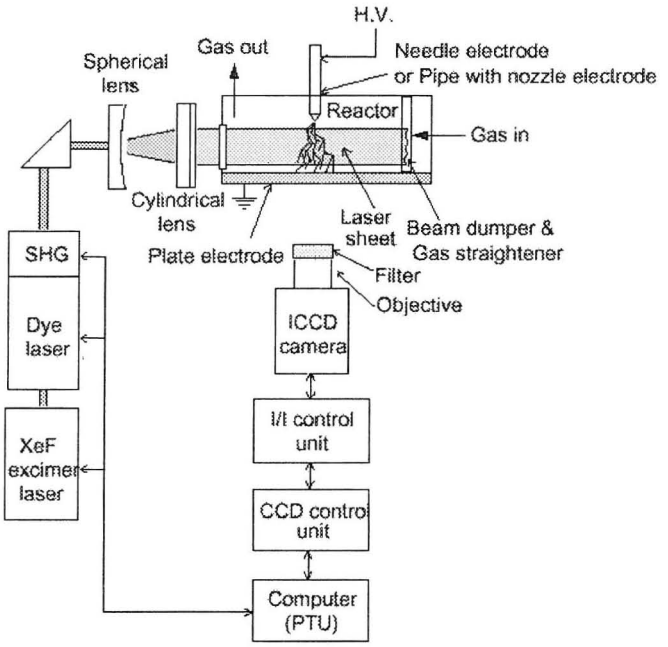

Fig. 1. Schematic diagram of the experimental apparatus.

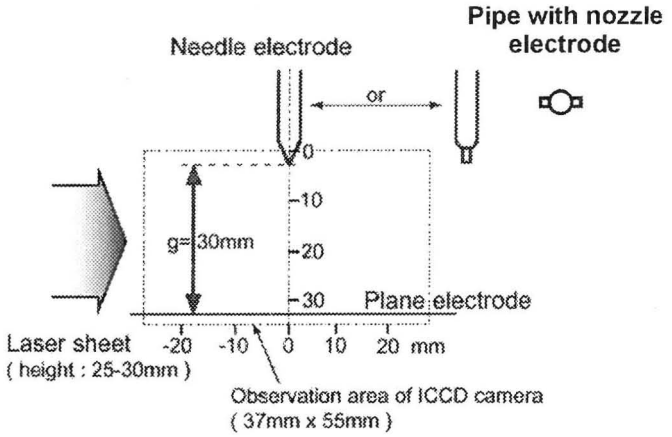

Fig. 2. Cross section of the discharge gap. ICCD camera observation area is indicated by the dashed rectangular.

LIF signal emitted at 90 degree to the laser sheet was imaged onto a gated ICCD camera (La Vision, Flame Star II) and two-dimensional distribution of NO molecules density around the discharge gap was recorded, and then processed by a computer. The area of the LIF measurement is illustrated in Fig. 2.

NO (up to 300 ppm)/air mixture flowed along the reactor with a flow rate of 0.2-3 L/min., which corresponds to a flow velocity of 0.4-6 mm/s. Concentrations of NO and NO_2 molecules at the inlet and outlet of the reactor were measured with a NO_x monitor (Hodakatest, Tests 33). This allowed the calibration of LIF signal in an absolute unit of NO concentration, i.e. in ppm. The experiment was carried out at room temperature and atmospheric pressure.

EXPERIMENTAL RESULTS AND DISCUSSION

In order to find the most suitable laser line for the monitoring of NO molecules, the laser wavelength was scanned through NO ($X^2\Pi(v''=0) \leftarrow A^2\Sigma^+(v'=0)$) transitions in the range of 225-227 nm and the corresponding NO fluorescence spectrum was recorded with the monochromator. Similarly, the LIF signal (proportional to the total NO fluorescence) was measured with the ICCD camera when the laser wavelength was scanned in the range of 225-227 nm. Both the highest intensities of the peaks in NO LIF spectrum and the strongest LIF signal were obtained for a laser wavelength, which, according to [20], corresponds to a laser wavelength of 226.192 nm. Therefore, the line wavelength of the LIF laser system used in these measurements was fixed as close as possible to 226.192

nm, to coincide with the highest intensity of the LIF signal. The calibration of NO LIF signal was carried out without discharge, when NO/air mixture with known concentration of NO molecules flowed through the reactor. A linear relationship between NO LIF intensity and NO concentration was observed up to NO concentration of about 250 ppm. This linear relationship was then used for determining NO concentration in the reactor and expressing it in an absolute unit (ppm) [21, 22].

TWO-DIMENSIONAL DISTRIBUTION OF NO MOLECULES IN THE NEEDLE-TO-PLATE REACTOR

Figs. 3 (a-c) show two-dimensional distributions of NO concentration in the vicinity of the electrode gap during DC corona discharge processing of a dry NO (200 ppm)/air mixture flowing with a velocity of 2 mm/s along the reactor (the corresponding gas flow rate – 1 L/min.). The intensity of the images shown in Fig. 3 corresponds to NO concentration (see NO concentration bar). At time (t = 0) the DC corona discharge started in the flowing gas, uniformly polluted with NO molecules [Fig. 3 (a)]. The discharge volume was approximately a cone with a base radius of 15 mm. After starting the corona discharge, NO LIF signal became weaker compared to that before the discharge. This indicated a decrease of NO concentration, i.e. NO removal from the processed gas mixture. However, astonishingly the NO concentration decrease was observed not only in the discharge and downstream regions of the reactor but also in the upstream vicinity of the discharge region [Fig. 3 (b)]. After about 4 minutes a steady state established (8 minutes is the residence time of the gas mixture in the reactor) and NO molecules were monitored only in the region below the needle electrode [Fig. 3 (c)]. However, their concentration there was much lower than their initial concentration (at t = 0). It is worth underlining that in the steady state NO molecules were almost absent also in the upstream vicinity of the discharge region.

The concentration of NO molecules is given in ppm, according to the calibration procedure. It is seen from Fig. 3 (c) that after establishing the steady state, the NO concentration in the discharge region increased with increasing distance from the needle (in the needle-to-plate direction). At this stage we cannot explain such a behaviour.

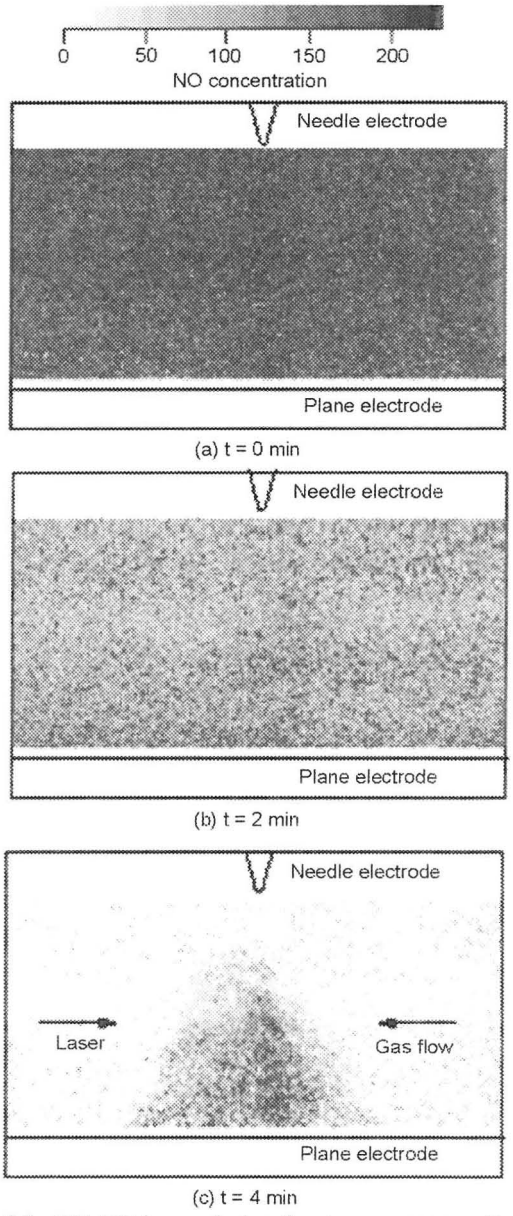

Fig. 3. Time evolution of the NO LIF image during the streamer corona discharge in the needle-to-plate reactor. The intensity of the images corresponds to NO concentration. Time t=0 min and t=4 min indicate the start of the discharge and the steady state, respectively. Operating gas: NO (200 ppm)/air, flow rate: 1 L/min, applied voltage: 21 kV.

We consider the observed removal of NO to be a result of oxidation NO to NO_2. This reasoning is justified by the increase of NO_2 concentration at the reactor outlet, measured with the NO_x monitor.

The reason of the astonishing decrease of the concentration of NO molecules in the upstream vicinity of the discharge region is not clear at this moment. In another experiment on the velocity field in the present reactor [24, 25], we found that the strong electrohydrodynamic (EHD) secondary flow from the stressed electrode towards both the upstream and downstream directions of the main flow occurs. This may suggest that the EHD secondary flow is capable of transporting long-living active species (e.g. O_3) from the discharge region into the upstream direction, where they may oxidize NO molecules in the reaction $NO + O_3 \rightarrow NO_2 + O_2$. This reaction is known to be the most efficient path of NO abatement in the chemical reactions occurring after the streamer pulse, in the time interval when the other active species, such as O, N, HO_2, and OH have already disappeared [7]. Another possible cause of the NO removal in the upstream vicinity of the discharge region, as suggested in [26], is direct photodissociation of NO molecules by the radiation of wavelengths shorter than $\lambda = 193$ nm, emitted by the discharge.

TWO-DIMENSIONAL DISTRIBUTION OF NO MOLECULES IN THE NOZZLE-TO-PLATE REACTOR

In the nozzle-to-plate reactor a stainless steel pipe with a nozzle (an inner and outer diameter of 1.0 mm and 1.5 mm, respectively), typical of the corona radical shower reactors [23], was used as the discharge electrode (Figs. 1 and 2). The counterelectrode and discharge gap were the same as in the case of the needle-to-plate reactor.

Figure 4 shows two-dimensional distributions of NO concentration in the nozzle-to-plate reactor during DC corona discharge processing of a dry NO (100 ppm)/air mixture flowing with a velocity of 6 mm/s along the reactor (the gas flow rate – 3 L/min.). The intensity of the images shown in Fig. 4 corresponds to NO concentration. It is seen from Fig. 4 that NO concentration decreases with increasing applied voltage. It is worth underlining that decomposition of NO molecules can be observed also in the upstream vicinity of the discharge region. In Figure 5 the two-dimensional distributions of NO concentration in the nozzle system-to-plate reactor during DC corona discharge processing of a dry NO/air mixture flowing along the reactor with applied voltage of about 36 kV are shown. This time decreasing of NO concentration in the upstream vicinity of the discharge region can also be observed. However, with increasing flow rate the upstream region of decreasing NO concentration become smaller.

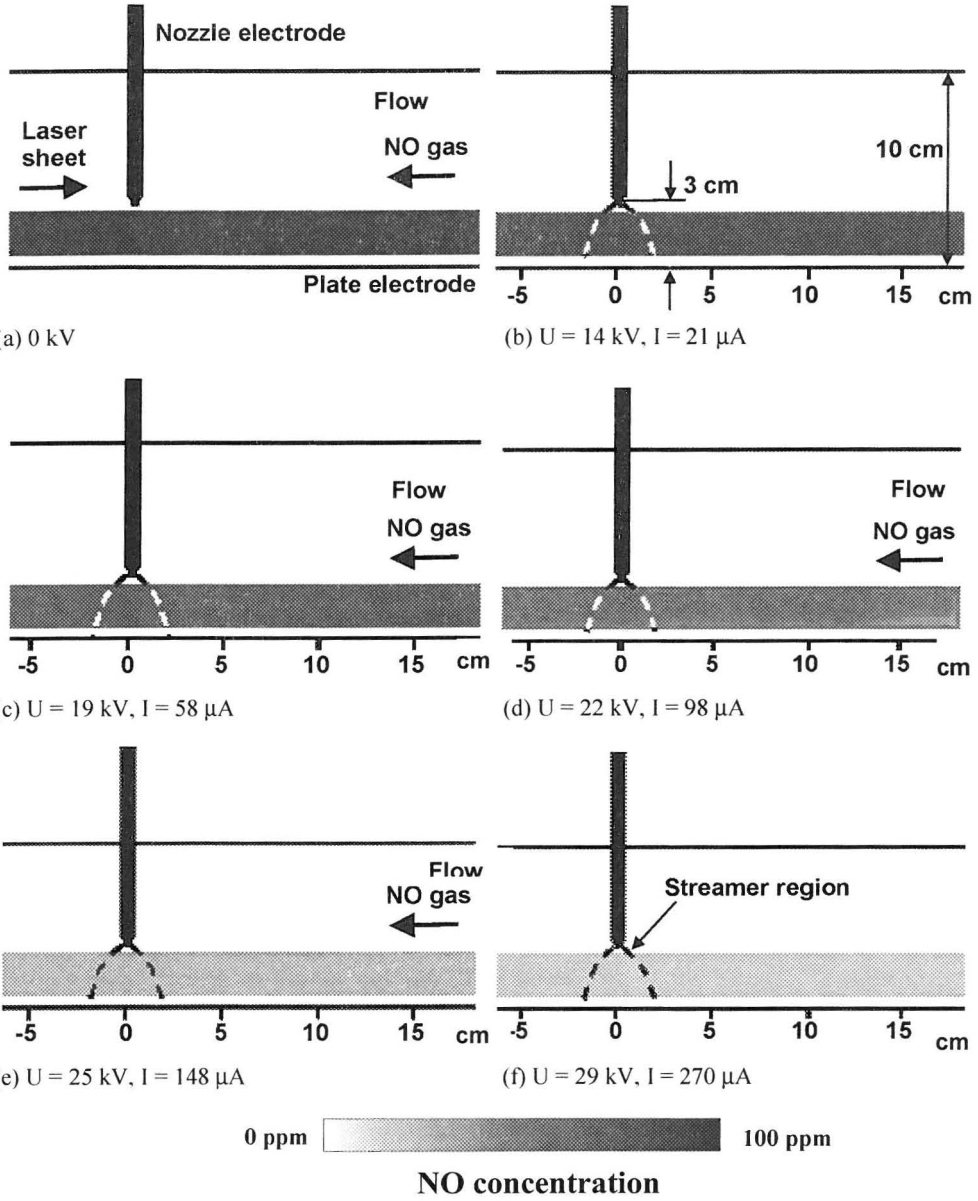

Fig. 4. Two-dimensional LIF observation of NO concentration in the upstream direction of the gas flow inside the nozzle-to-plate reactor. The intensity of the images corresponds to NO concentration, as in the NO concentration bar. Operating gas: NO (100ppm)/air, flow rate: 3L/m.

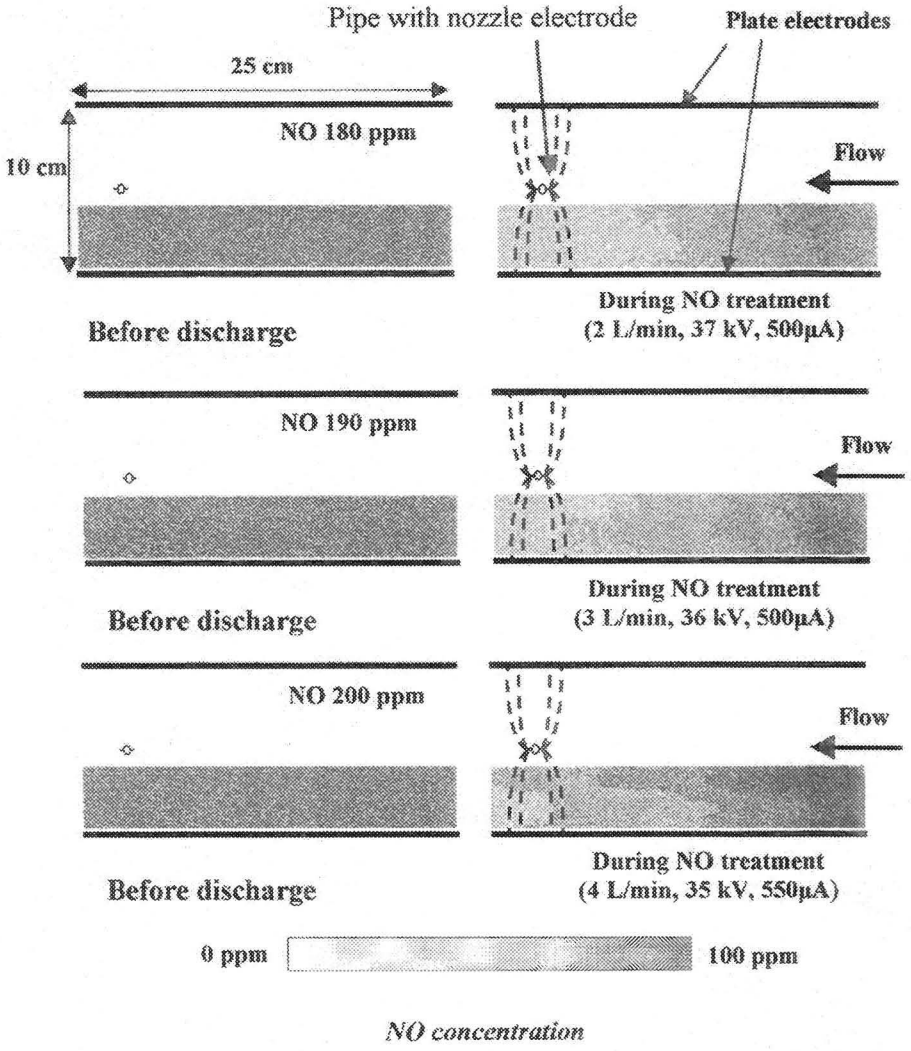

Fig. 5. Two-dimensional LIF observation of NO concentration in the upstream direction of the gas flow inside the nozzle system-to-plate reactor. The intensity of the images corresponds to NO concentration, as in the NO concentration bar. Operating gas: NO/air, applied voltage: 36 kV.

This investigation showed that the process of NO removal by corona discharges can occur not only in the paths of the corona streamers or in their adjacent vicinity but can be more spatially distributed, also in the upstream

direction of the flue gas flow. This has to be taken into account when modelling the kinetics of plasma-chemistry processing of NO_x pollutants by the corona discharges and designing the reactors.

SUMMARY AND CONCLUSIONS

The measurements of two-dimensional NO concentration in the non-thermal plasma reactor, in which the positive DC corona discharges occurred between either the needle-to plane or nozzle-to-plate electrode, were carried out using LIF diagnostic technique.

The obtained results can be summarized as follows:

1. The LIF was proved to be a powerful space- and time-resolved diagnostic method for *in-situ* and real-time two-dimensional observation of the corona-discharge induced abatement of NO molecules in the non-thermal plasma reactors.
2. In the positive DC corona discharges in the non-thermal plasma reactors, additional corona streamers are induced by the UV laser sheet pulses shot into the electrode gap for LIF NO detection. The light emitted by these streamers may hinder the LIF signal detection. Fortunately, the separate detection of the LIF signal and the light emitted by the laser-induced streamer is possible, if an appropriate adjusting of the recording delay and exposure time of the ICCD camera is set.
3. The results of the measuring of the two-dimensional concentration of the ground-state NO molecules in the non-thermal plasma reactor showed an efficient removal of NO molecules from NO (200 ppm)/air mixture by the corona discharge, regardless the electrode arrangement. In the steady-state condition the concentration of NO molecules decreased not only in the discharge and downstream regions of the reactor but also in the upstream vicinity of the discharge region. This suggests that the EHD flow enhanced the NO removal in the reactor. To clarify this phenomenon more investigation is needed.
4. The increase of NO_2 concentration at the reactor outlet, measured by the NO_x monitor, suggests that the observed removal of NO is a result of oxidation NO to NO_2 in the reactor.

REFERENCES

1. **Alekseev G. Yu., Levchenko A V., Bityurin V.**, "Flue gas cleaning by pulsed corona. Part II: Chemical kinetics and heat/mass transfer in NO/SO_2 removal", Research Report, EG/93/673, Eindhoven University of Technology, 1993.
2. **Gentile A. C., Kushner M. J.**, J. Appl. Phys., 78, 3, 2074-2085, 1995.
3. **Eichwald O., Yousfi M., Hennad A.**, Benabdessadok M. D., J. Appl. Phys., 82, 4781-4794, 1997.
4. **Marode E., Samson S., Djermoune D., Deschamps N., Touzeau M.**, "Influence of temperature, hydrodynamic and diffusion process on the chemical activity in transient filamentary discharge", Proceedings of the 2nd Int. Symp. on Non-Thermal Plasma Technology for Pollution Control, Salvador, Brazil, pp. 130-135, 1997.
5. **Kulikovsky** A. A., IEEE Trans. Plasma Sci., 26, 4, 1339-1346, 1998.
6. **Chang J.- S., Kwan A.**, „Modelling of Dry Air Chemistry in a Coaxial Wire-Pipe Negative Corona Discharge", Proceedings of ESA-IEJ Joint Symposium on Electrostatics, Palo Alto, California, pp. 391-407, 1998.
7. **Mizeraczyk J., Dors M., Nichipor G.V.**, J. Adv. Oxid. Technol., 4, 380-385, 1999.
8. **Rothe E. W., Andresen P.**, Appl. Optics, 36, 18, 3971-4033, 1997.
9. **Chang J.- S., Lawless P.A., Yamamoto T.**, IEEE Trans. Plasma Sc., 19, 1152-1167, 1991.
10. **Penetrante B. M., Schultheis S. E. ed.**, "Non-Thermal Plasma Techniques for Pollution Control", Springer-Verlag, 1993.
11. **Ershov A., Borysov J.**, J. Phys. D: Appl. Phys., 28, 68-74, 1995.
12. **Coogan J. J.; Sappey A. D.**, IEEE Trans. Plasma Sc., 24, 91-92, 1996.
13. **Ono R., Oda T.**, "Two dimensional measurement of OH radicals generated by discharge plasma by using tunable excimer laser induced fluorescence", Proceedings of the Asia-Pacific Workshop on Water and Air Treatment by Advanced Oxidation Technologies: Innovation and Commercial Applications, Tsukuba, Japan, pp. 66-69, 1998.
14. **Ono R., Oda T.**, " Measurement of hydroxyl radicals in an atmospheric pressure discharge plasma by using laser-induced fluorescence", IEEE Trans. Ind. Appl., 36, 1, 82-86, 2000.
15. **Ono R., Oda T.**, "Measurement of hydroxyl radicals in pulsed corona discharge", Proceedings of the IEJ-ESA Joint Symp. on Electrost., Kyoto, Japan, pp. 287-296, 2000.
16. **Hazama H., Fujiwara M., Sone T., Hashimoyo H., Ishida M., Tanimoto M.**, "Fluorescence imaging of NO in a pulsed corona discharge reactor ", Proceedings of the Asia-Pacific Workshop on Water and Air Treatment by Advanced Oxidation Technologies: Innovation and Commercial Applications, Tsukuba, Japan, pp. 70-73, 1998.
17. **Roth G. J., Gundersen M. A.**, IEEE Trans. Plasma Sci., 27, 28-29, 1999.
18. **Tochikubo F., Watanabe T.**, "Two-dimensional measurement of emission intensity and NO density in pulsed corona discharge", HAKONE VII Internationa Symposium on High Pressure Low Temperature Plasma Chemistry: , Greifswald, Germany, pp.219-223, 2000.
19. **Fresnet F., Baravian G., Pasquiers S., Postel C., Puech V., Rousseau A., Rozoy M.**, J. Phys. D: Appl. Phys., 33, 1315-1322, 2000.
20. **Luque J.**, "Spectroscopic database and spectral simulation for OH, CH, CN, NO, SiH and CF (Version 1.61)", SRI International, 1999.
21. **Mizeraczyk J., Ohkubo T., Kanazawa S., Nomoto Y.**, "Features of DC corona discharge streamers induced by a UV (248 nm) laser sheet", Proceedings of 1999 Annual Meeting of the Institute of Electrostatics Japan, Thudanuma, Japan, pp. 231-234, 1999.
22. **Ohkubo T., Akamine S., Kanazawa S., Nomoto Y., Mizeraczyk J.**, "Streamer corona discharge induced by a laser Ppulse in a needle-to-plate electrode system and the related NO concentration distribution", Proceedings of the First Polish-Japanese Hakone Group

Symposium on Non-thermal Plasma Processing of Water and Air, Sopot, Ed.: J. Mizeraczyk, M. Dors, pp. 85-88, 2000.
23. **Ohkubo T.; Kanazawa S., Nomoto Y., Chang J.-S., Adachi T.**, "Time dependence of NO_x removal rate by a corona radical shower system", IEEE Trans. Ind. Applicat., 32, pp. 1058-1062, 1996.
24. **Kanazawa S., Ohkubo T., Ito T., Shuto Y., Nomoto Y., Mizeraczyk J.**, "LIF diagnostics of NO molecules in atmospheric-pressure DC streamer coronas used for NOx abatement", APP Spring Meeting, Bad Honnef 2001,Germany, Diagnostics of Non-equilibrium High Pressure Plasmas, Book of Papers, pp. 205-208, 2001.
25. **Mizeraczyk J., Kocik M., , Dekowski J., Dors M., Podlinski J., Ohkubo T., Kanazawa S., Kawasaki T.**, J. Electrostatics, 51-52, 272-277, 2001.
26. **Spaan M., Leistikov J., Schulz-von der Gathen V., Döbele H.F.**, Plasma Sources Sci. Technol., 9, 146-151, 2000.

ZASTOSOWANIE TECHNIKI LIF DLA OBSERWACJI CZASOWO-PRZESTRZENNEJ ROZKŁADU ZANIECZYSZCZEŃ GAZOWYCH W REAKTORACH PLAZMY NIERÓWNOWAGOWEJ

J. Mizeraczyk[1], T. Ohkubo[2], S. Kanazawa[2], M. Kocik[1]

[1]Ośrodek Techniki Plazmowej i Laserowej, Instytut Maszyn Przepływowych PAN, 80-231 Gdańsk, Fiszera 14, Polska jmiz@imp.gda.pl
[2]Department of Electrical and Electronic Engineering, Oita University,700 Dannoharu, Oita, Japan 870-1192, tohkubo@cc.oita-u.ac.jp

S t r e s z c z e n i e. Technika pomiarowa oparta na fluorescencji wymuszonej promieniowaniem laserowym (LIF) wspomagana przez detekcję wzmacnianego CCD sygnału świetlnego i szybką cyfrową obróbkę obrazu jest efektywną metodą diagnostyczną do in-situ dwuwymiarowej obserwacji plazmowych procesów chemicznych odpowiedzialnych za rozkład NO_x ($NO + NO_2$) w reaktorach plazmy nierównowagowej. W prezentowanej pracy przedstawiono dwuwymiarowy rozkład stężeń cząstek NO w stanie podstawowym wewnątrz reaktora podczas wyładowań w syntetycznym gazie spalinowym (stężenie NO do 300ppm). Pokazano, że dzięki efektowi EHD, proces utleniana NO może zachodzić również w obszarze przed wyładowaniami, co należy uwzględnić w modelowaniu i projektowaniu reaktorów plazmowych.

S ł o w a k l u c z o w e : diagnostyka LIF, wyładowania koronowe, NO_x , usuwanie NO_x, reaktor plazmy nierównowagowej.